Article

Cobalt Biosorption in Fixed-Bed Column Using Greenhouse Crop Residue as Natural Sorbent

Gabriel Blázquez [ID], María Ángeles Martín-Lara *[ID], Irene Iáñez-Rodríguez, Inés Morales, Antonio Pérez [ID] and Mónica Calero

Chemical Engineering Department, Faculty of Sciences, University of Granada, 18071 Granada, Spain
* Correspondence: marianml@ugr.es; Tel.: +34-958240445

Abstract: Intensive greenhouse agriculture annually produces large amounts of residues. The present work focused on the study of the dynamic adsorption of cobalt from aqueous solutions over a vegetal residue from intensive greenhouse cultivation. The influence of three operating variables, feed-flow rate, inlet concentration of cobalt and bed height, was analyzed. According to the results, the variable that particularly affected the percentage of cobalt adsorbed was the feed-flow rate. The results were also fitted to an adaptive neuro fuzzy system (ANFIS) model to predict cobalt adsorption from aqueous solutions and choose the most favorable operating conditions. Results were evaluated using root mean squared error (RMSE), coefficient of determination (R2) and other typical statistic factors as performance parameters. The experimental and model outputs displayed acceptable result for ANFIS, providing R^2 values higher than 0.999 for both cobalt removal (%) and biosorption capacity (mg/g). In addition, the results showed that the best operating conditions to maximize the removal of cobalt were 4 mL/min of feed-flow rate, 25 mg/L of inlet concentration and 11.5 cm of bed-height.

Keywords: adaptive neuro fuzzy system; biosorption; cobalt; fixed-bed column; greenhouse crop residue

1. Introduction

Industrial development has led to the massive generation of different types of waste. Specifically, intensive greenhouse agriculture annually produces large amounts of greenhouse crop residue (GCR). The recovery of this waste is essential, since it has environmental and economic benefits.

On the other hand, there is another problem that derives from industrial activity: the contamination of aquatic resources. Some industries, such as chemical, metallurgical, mining, and electrical and electronics, pour large amounts of heavy metals into water; these are considered highly toxic pollutants even at low concentrations, due to their non-degradable nature [1]. Some of these heavy metals are lead, cadmium, zinc, nickel, copper, mercury, chromium, cobalt, and iron. All of them cause health and environmental problems [2]. Cobalt is a heavy metal that has many applications: as a catalyst to synthesize fuels or alcohols, additive for paints, synthesis of alloys with high thermal stability or in medicine as a source of gamma rays. Although it is an element that, in small amounts, has beneficial effects on health, it can also produce very harmful effects, such as asthma, heart failure and damage to the thyroid and liver, and exposure to ionizing radiation is related to an increase in the risk of developing cancer [3,4].

The removal of heavy metals can be carried out through a wide range of technologies such as chemical precipitation, adsorption, membrane filtration, oxidation, ozonation, ion exchange and electrodialysis [5,6]. However, these methods have some drawbacks, including sensitive operating conditions, poor removal, and high energy requirements [6]. One of the most promising technologies for the removal of heavy-metal ions from dilute water effluents is adsorption using novel economical and environmentally friendly bioadsorbents (a technology often called biosorption). A wide range of different materials such as walnut

shells [7], coffee husk [8], pineapple husk [9], olive stone [10], melon peel [11], eggshell wastes [12] or mushroom compost [13], among others, have been used as biosorbent or bioadsorbent materials for heavy-metals removal.

Regarding the biosorption process, it can be carried out continuously or discontinuously. The discontinuous mode is normally used to obtain the main parameters of the process such as the biosorption capacity, the possibility of regeneration of the biomass and the optimal experimental conditions [14]. However, continuous experiments are used to scale the process from the laboratory scale to the industrial scale and are simple and low-cost studies [15]. The combination of both modes of operation is a complete study of the biosorption process for the selected material.

On the other hand, the combination of artificial neural networks (ANNs) and fuzzy logic systems (FS) creates a powerful tool to reliably predict the behavior of complex nonlinear systems. The adaptive neuro-fuzzy inference system (ANFIS) has been previously applied to different biosorption systems to determine the influence of operating variables on the removal of metals from water. For example, Ronda et al. [16] applied the ANFIS model to lead biosorption using olive stone. Fawzy et al. [17,18] used it to model the batch biosorption of cadmium and nickel over different types of biomasses, or Bingöl et al. [19] used the ANFIS in the copper biosorption modeling onto date palm.

The ANFIS design is comprised of a five-layered neural network that uses fuzzy inference system concepts. It has advantages compared to other modeling tools. For example, it offers quite high goodness of fit and allows the study of the influence of each of the operating parameters [20].

The present work focused on the study of the continuous cobalt biosorption process using a residue from intensive greenhouse cultivation. The influence of three variables in the process (bed height, flow rate and initial concentration of cobalt) was analyzed. The results were adjusted to the ANFIS model, which made it possible to define the most favorable operating conditions in a biosorption column for this material and this metal. The greatest novelty of this work is the material used for the cobalt removal process, which has not been tested as a biosorbent in any previous study.

2. Materials and Methods

2.1. Material

The material used is a waste from intensive greenhouse cultivation provided by a vegetable waste treatment plant located in Motril, Granada (Spain). The biomass obtained (namely, GCR) was ground using a blade mill (IKA MF-10) and was sieved selecting the fraction with a size between 0.250 mm and 1.00 mm.

A complete characterization of the material was carried out in a previous work [21]. Table 1 summarizes the main characteristics of the material.

Table 1. Main characteristics of the biosorbent material.

Analysis		Value
pH_{pzc}		7.35
Elemental analysis	%C	34.02
	%H	5.89
	%N	3.15
	%O (by difference considering ash content)	32.95
Immediate or proximate analysis	Moisture, %	7.43
	Volatile matter, %	56.66
	Fixed carbon, %	11.95
	Ash, %	23.97
Surface properties analysis	BET surface area, m^2/g	6.2
	Pore volume, cm^3/g	0.0073
	Average pore size, Å	47.5

Table 1. *Cont.*

Analysis	Value
FTIR analysis	–OH (3330 cm^{-1}) CH– (2760 y 2980 cm^{-1}) C=O (1730 cm^{-1}) Aromatic vibration of lignin (1620 cm^{-1}) Functional groups located in lignin (1509 y 1200 cm^{-1})

2.2. Column Biosorption Tests

The behavior of cobalt biosorption in a fixed-bed column was studied for the native residue. Different operating conditions were analyzed, obtaining the rupture curves that would later serve to choose the best operating conditions for the process.

The breakthrough curve shows the behavior of a fixed-bed column from the point of view of the amount of metal that can be retained and, usually, it is expressed in terms of a normalized concentration defined as the quotient between the metal concentrations in the liquid at the outlet and inlet of the column (C/C_i), as a function of time or effluent volume for a fixed-bed height. The effluent volume, V_{ef} (mL), can be calculated using the following equation:

$$V_{ef} = Q \cdot t_{total} \tag{1}$$

where t_{total} is the total time in minutes and Q is the feed-flow rate that circulates through the column in mL/min.

The area under the breakthrough curve, between the appropriate limits, represents the total amount of metal retained (or maximum column capacity), q_{total}, in mg, for a given concentration of the feed and can be determined by integration as follows:

$$q_{total} = \frac{Q}{1000} \int_{t=0}^{t=t_{total}} C_R dt \tag{2}$$

where C_R is the concentration of metal retained in mg/L.

Regarding the limits, we considered the total time as the time of saturation (when $C/C_i \geq 0.95$) and the initial time the starting point of the experiment.

The total amount of metal that passes through the column, m_{total} in mg, can be calculated using the following expression:

$$m_{total} = \frac{C_i \cdot Q \cdot t_{total}}{1000} \tag{3}$$

In addition, therefore, the total percentage of metal retained (%R) during the operation would be obtained as:

$$\%R = \frac{q_{total}}{m_{total}} \cdot 100 \tag{4}$$

As in batch processes, column equilibrium studies require knowledge of the adsorption capacity, q_e, (mg of adsorbed metal/g of biosorbent), and the concentration of metal that remains in a solution when equilibrium is reached, C_e (mg/L), and can be determined by the following expressions, respectively:

$$q_e = \frac{q_{total}}{m} \tag{5}$$

$$C_e = \frac{m_{total} - q_{total}}{V_{ef}} \cdot 1000 \tag{6}$$

where m represents the mass of biosorbent in the column.

All the parameters previously described allow comparing and analyzing the differences between the behaviors of the column when the operating conditions change.

All biosorption experiments were carried out in a fixed-bed column of 13 cm in height and 1.3 cm internal diameter. The column operated with an upward flow fed by a Dinko peristaltic pump, model D-21V. The solution entered the column from a 2 L tank. To carry out the experiments, two different amounts of biosorbent were introduced into the column (1 and 2 g). The column was filled with the required number of glass balls at the bottom and a layer of cotton wool to prevent the biosorbent from getting between the glass balls. The solution with the desired concentration of cobalt (12.5 and 25 mg/L) was fed upwards by means of a peristaltic pump using a fixed feed-flow rate (2 and 4 mL/min). Samples were collected from the top of the column and cobalt concentration was analyzed. The pH at which all the experiments were carried out was that of the solution (around 6.5). The determination of the cobalt content of the samples was carried out by atomic absorption spectrophotometry, using Perkin–Elmer AAnalist 200 equipment.

To predict the behavior of the column, the Thomas model was used. The Thomas model is one of the most commonly used methods and is based on second-order kinetics, considering that sorption is controlled by mass transfer at the interface. It can be used to describe the entire breakthrough curve, especially between the breakthrough and saturation times [22]. The Thomas model can be expressed by the following equation:

$$\frac{C}{C_i} = \frac{1}{1 + exp\left(\frac{k_{Th}}{Q}\left(q_0 m - C_i V_{ef}\right)\right)} \tag{7}$$

where k_{Th} is the Thomas constant, related to mass transfer, mL/mg·min; q_0 is the equilibrium adsorption capacity, mg/g; and V_{ef} is the effluent volume in L.

In addition, two-level full factorial design for three factors, namely, feed-flow rate (factor A), inlet cobalt concentration (factor B) and bed height (factor C) was performed by triplicate.

2.3. Optimization of the Operating Conditions in Continuous Biosorption by ANFIS Model

The ANFIS model was applied in this work to two different response variables: the removal percentage or retained metal percentage (%R) and the biosorption capacity (q_e). As two levels were used for each of the three input variables (feed-flow rate, inlet cobalt concentration and height bed), application of ANFIS resulted in a model with 8 constants. In addition, three points outside of operating conditions were also used as testing points (Table S2). A summary is reported below. More details of ANFIS model can be found in Supplementary Materials. Finally, to implement and test the ANFIS, the "Matlab ANFIS Edit Tool" was used.

The response variable, y, was calculated using the following equation:

$$y = \frac{\sum_{l=1}^{8} a_l \cdot FR_l}{\sum_{l=1}^{8} FR_l} \tag{8}$$

where a_l represents the single constant parameters (one per variable and level). Moreover, each FR_l is the combination of levels (low and high) for each variable (the feed-flow rate, the inlet concentration, and the bed height).

The Gaussian equations for the two levels (low and high) are defined as follows:

$$\mu(low) = exp\left(-0.5 \cdot \left(\frac{x - x_{low}}{L}\right)^2\right) \tag{9}$$

$$\mu(high) = exp\left(-0.5 \cdot \left(\frac{x - x_{high}}{L}\right)^2\right) \tag{10}$$

where L is the width of the Gaussian function distribution and x_{low} and x_{high} are the values of each level (low and high) for each variable.

Taking all previous considerations into account, the equation for the calculation of the response variable can be simplified and expressed as:

$$y = \frac{a_1 \cdot FR_1 + a_2 \cdot FR_2 + \ldots + a_7 \cdot FR_7 + a_8 \cdot FR_8}{FR_1 + FR_2 + \ldots + FR_7 + FR_8} \quad (11)$$

3. Results and Discussion

3.1. Column Biosorption Tests

Firstly, the influence of the main operating variables on the breakdown curves was analyzed: feed-flow rate, inlet cobalt concentration and mass of biosorbent used (or bed height). Figure 1 shows the effect of the operating variables on the breakthrough curves for cobalt biosorption onto GCR and Table 2 shows the calculated characteristic parameters of these breakthrough curves.
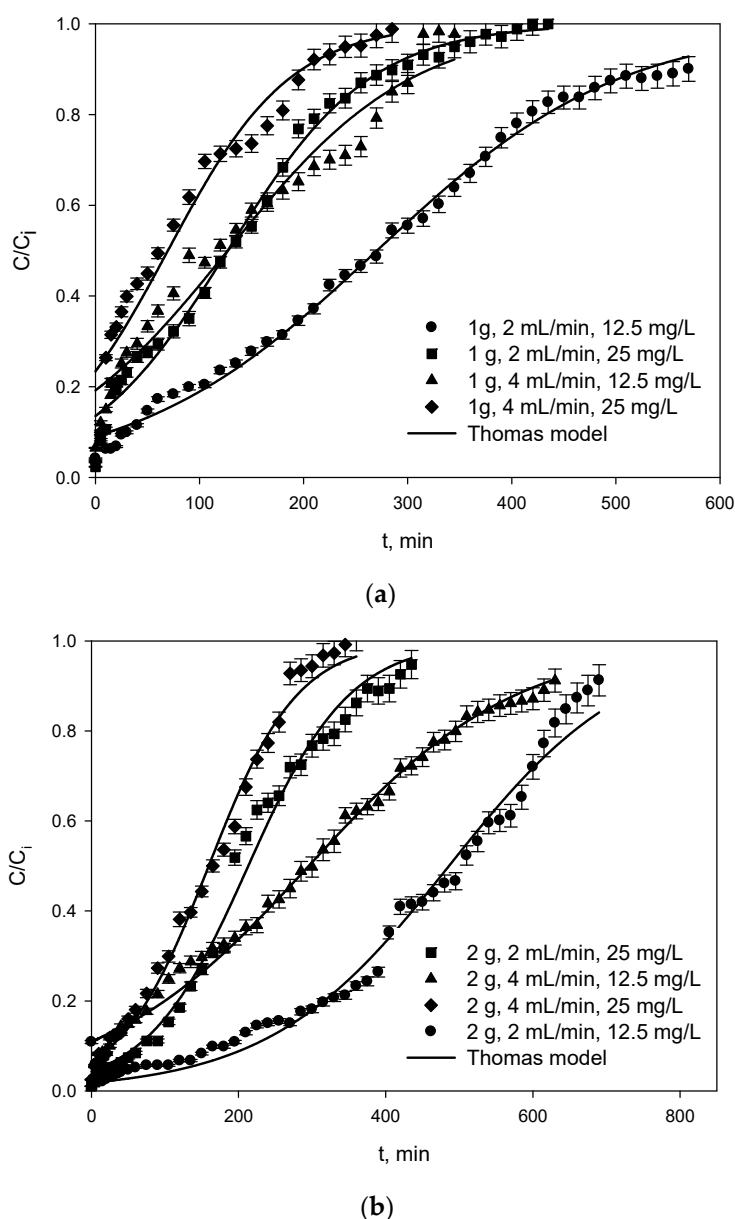

(**a**)

(**b**)

Figure 1. (**a**) Breakthrough curves for cobalt biosorption onto GCR (height of 5 cm). (**b**) Breakthrough curves for cobalt biosorption onto GCR (height of 11.5 cm).

Table 2. Main parameters of the breakthrough curves for the different operating conditions.

Bed Height, cm	Feed-flow Rate, mL/min	Inlet Cobalt Concentration, mg/L	%R	q_{total}, mg	m_{total}, mg	V_{ef}, mL	q_{eq}, mg/g	C_{eq}, mg/L	t_S, min
5 (1 g)	2	25	31.6	7.3	23.1	870	7.3	18.2	435
		12.5	47.8	7.3	15.2	1140	7.3	7.0	570
	4	25	30.0	9.1	30.4	1140	9.1	18.7	285
		12.5	39.5	7.9	20.0	1380	7.9	8.7	345
11.5 (2 g)	2	25	50.1	11.5	23.0	870	5.8	13.2	435
		12.5	73.7	13.7	18.6	1380	6.9	1.8	690
	4	25	43.5	17.0	39.1	1440	8.6	11.8	360
		12.5	52.7	19.1	36.9	2520	9.5	7.1	630

According to the results, the saturation of the column was achieved in all cases except for the lowest concentration (12.5 mg/L) and the highest amount of biosorbent (2 g). In general, an increase in the feed-flow rate caused an increase in the feed amount of cobalt, resulting in a faster saturation of the column and a decrease in the saturation time. It is also observed that an increase in the inlet feed flow produced a decrease in the cobalt removal percentage. When a higher flow rate was used, the contact time between the cobalt and biosorbent was decreased and a lower removal percentage was observed. For example, for a concentration of 25 mg/L and a biosorbent mass of 1 g, the removal percentage decreased from 31.56% to 23.53% when the feed-flow rate increased from 2 to 4 mL/min. However, the biosorption capacity increases with feed-flow rate, especially when a biosorbent mass of 2 g is used. On the other hand, an increase in inlet cobalt concentration produced a higher amount of cobalt feed to the column and, consequently, a reduction in the time to achieve saturation, since the sites of the biosorbent were quickly occupied by cobalt and a shorter time was required to reach the saturation point. For example, in the case of using 1 g of material and a flow rate of 2 mL/min, the saturation time for the highest concentration (25 mg/L) was 300 min while for the lowest concentration (12.5 mg/L) it was 570 min. Finally, if the effect of bed height was analyzed, saturation time and the total amount of cobalt retained increased with increasing bed height. In addition, the total amount of cobalt retained (q_{total}) and the removal percentage increased when the amount of biosorbent (bed height) was increased. This was due to the growth in the biosorption zone in the fixed-bed column. Consequently, there were more sites available for biosorption, that is, there was a greater contact surface, which led greater metal retention [23,24].

These results agreed with those found by other authors in similar studies with other metals and biosorbent materials [9,25–27]. Amin et al. [25], studying the biosorption of Cu(II) and Pb(II) by raw and treated date palm leaves and orange peel, found that both breakthrough and exhaust times increased with increasing the bed height of the fixed-bed column and decreased with increasing initial metal concentration, particle size, and flow rate. Hymavathi and Prabhakar [26] studied cobalt and lead adsorption by *Ficus benghalenesis* L. in a fixed-bed column, finding that the highest adsorption capacities (11.09 mg/g for cobalt and 12.27 mg/g for lead) were obtained using 20 mg/L of metal solution at 1.0 mL/min of flow rate and 2 cm of bed height. Yahya et al. [28] studied Cu (I) and Cr ions adsorption using almond shell in a fixed-bed column. These authors found that the optimal conditions were a flow rate of 3.0 mL/min, bed height of 7.0 cm, inlet concentrations of 7.0 mg/L and 67.5 mg/L for Cu(II) and Cr ions, respectively. Under these conditions, the percentage removal of Cu (II) and Cr ions was 70.0 and 65.9% and adsorption capacity value was 2.41 mg/g and 21.92 mg/g, respectively.

On the other hand, the breakthrough curves obtained (Figure 1) were fitted to the Thomas model. The results of the model parameters are shown in Table 3.

Table 3. Constants of the Thomas model for the fitting of the breakthrough curves.

Bed Height, cm	Feed-flow Rate, mL/min	Inlet Cobalt Concentration, mg/L	k_{Th}, mL/mg/min	q_0, mg/g	R^2	$\Sigma(q_{exp} - q_{cal})^2$
5 (1 g)	2	25	0.54	6.7	0.990	0.032
		12.5	0.64	7.2	0.995	0.017
	4	25	0.63	7.4	0.953	0.092
		12.5	0.76	7.6	0.961	0.082
11.5 (2 g)	2	25	0.55	5.7	0.989	0.045
		12.5	0.60	6.6	0.985	0.061
	4	25	0.61	8.5	0.992	0.027
		12.5	0.68	8.9	0.990	0.038

Thomas's model fits the experimental results well with R^2 values close to 0.99 in most cases, showing that diffusion is not the limiting stage [28]. The adsorption capacity values of the Thomas model are similar to those obtained experimentally, although slightly lower in some cases, which may be because the Thomas model is not appropriate for full breakthrough-curve fitting, resulting in errors, especially at lower or higher time periods of the breakthrough curve. The constant k_{Th} generally increases with increasing flow and decreases slightly with increasing bed height. In addition, the constant k_{Th} tends to decrease with increasing initial cobalt concentration, which could indicate that the system is controlled by external mass transfer in the initial part of the curve [28]. Researchers found different results depending on the biosorbent–adsorbate system studied. Yahya et al. [28] found that the Thomas model fits well the breakthrough curve in the biosorption of Cr and Cu (II) ions from industrial tannery effluent using almond shell. These authors indicate that k_{Th} decreases with increasing flow and initial metal concentration and increases with increasing bed height.

Homen et al. [29] studied the use of *Moringa oleifera* residues for herbicide atrazine removal, obtaining that the Thomas model fits the experimental data in all the conditions used. The value of the constant k_{Th} increases when the flow rate increases, which suggests faster bed saturation. In addition, these authors found that when the initial concentration increases, the values of k_{Th} and q_0 decrease.

Amin et al. [25], studying the biosorption of copper and lead with raw date palm leaves, found that k_{Th} decreases when the initial concentration of metal increases, which they attribute to an increase in the driving force due to the difference between the concentration of ions on the surface of the solid and solution. These authors also indicated a slight decrease in k_{Th} and q_0 with increasing bed height, which they attribute to the fact that the metal ion concentration ratio increased more quickly in the smaller bed, indicating that a lower bed height improves the adsorption of metals, although the bed is saturated more quickly. This is similar to what occurs in this work (Table 3) for a flow rate of 2 mL/min.

3.2. Optimization of Operating Conditions in Continuous Biosorption Using ANFIS Model

Once the effect of the variables was analyzed individually, ANFIS was used to predict and optimize the removal of cobalt by GCR. After the experimental data were entered in the ANFIS edit tool, the following constants (Table 3) and parameters (Table 4) data were obtained. In addition, datasets for training and testing the model are provided in Table S2 of Supplementary Materials.

The data reported in Table 4 correspond to the model constants for cobalt removal (%R) and cobalt biosorption capacity (q_e, mg/g) and were calculated using Equation (10) (Equation (S6) in the Supplementary Material). These constants indicate the value of the response variable if you work under the conditions of the corresponding rule (see the rules in the Supplementary Material). The rest of the model parameters are reported in Table 5 and correspond to Formulas (8) and (9) (Equations (S3) and (S4) in Supplementary Materials).

Table 4. Constants of the ANFIS model for the %R and q_e fitting.

Constant	%R	q_e
a_1	46.38	7.267
a_2	76.17	6.719
a_3	28.83	7.229
a_4	49.09	5.403
a_5	37.18	7.805
a_6	46.01	9.891
a_7	16.91	8.831
a_8	53.40	8.349

Table 5. Parameters of the ANFIS model for the %R and q_e fitting.

Variable	Level	X		L	
		%R	q_e	%R	q_e
Feed-flow rate	Low	2.180	1.993	1.1900	0.8330
Feed-flow rate	High	4.089	3.995	0.6425	0.8607
Concentration	Low	12.52	12.50	5.3590	5.3090
Concentration	High	25.04	25.00	5.2180	5.3080
Bed-height	Low	4.900	5.000	2.5140	2.7600
Bed-height	High	11.43	11.50	2.9180	2.7600

Table 6 shows the experimental and calculated values as well as the relative error and R^2 values for each studied response variable.

Table 6. Experimental and calculated values and relative error of the model for the metal retained percentage (%R) and biosorption capacity (q_e).

%R			q_e		
Experimental	Calculated	Error (%)	Experimental	Calculated	Error (%)
31.56	31.56	0.003	7.29	7.290	0.003
47.77	47.77	0.010	7.28	7.280	0.005
30.01	30.01	0.006	9.13	9.129	0.013
39.54	39.54	0.008	7.94	7.940	0.002
50.14	50.14	0.003	5.77	5.769	0.011
73.69	73.69	0.007	6.87	6.870	0.004
43.45	43.45	0.004	8.59	8.593	0.205
52.71	52.71	0.007	9.53	9.529	0.011
	$R^2 > 0.999$			$R^2 > 0.999$	

The goodness of fitting was very high for both analysed responses, showing R^2 values higher than 0.999 and relative errors lower than 0.013.

To visualize the most favourable operating conditions for the biosorption process, surface graphs were generated in which the maximum points can be clearly observed. Figures 2 and 3 show the graphs obtained for the percentage retained and biosorption capacity, respectively.

The variable that most affected the percentage of adsorbed metal is the flow rate. The most favorable operating conditions to maximize the percentage of metal retained were 2 mL/min feed-flow rate, 12.5 mg/L of inlet concentration and 11.5 cm of bed height. In

addition, if the feed-flow rate is kept constant at any value, the variable that most affects is the bed height, with the yield being higher for heights of 11.5 cm.

The most favorable operating conditions considering the biosorbent capacity of the material are a feed-flow rate of 4 mL/min, a concentration of 12.5 mg/L and a bed height of 11.5 cm. Again, the variable that most influenced the biosorbent capacity was the flow rate. It was observed that the shape of the response surface changed completely when the flow rate was changed from 2 to 4 mL/min.

Again, when the feed-flow rate is kept constant, the bed height is the most influential variable, taking q_e maximum values when the bed height is 11.5 cm.

Some researchers have carried out similar studies to optimize the adsorption process of different contaminants in a packed column. Hanumanthy et al. [30] optimized the operating conditions for the adsorption of Remazol Brilliant Orange 3R (RBO3R) in a packed-bed column using the RSM and ANFIS model. These authors found that the removal efficiency was decreased when sorbent depth increased and initial RBO3R concentration was decreased. In addition, the removal efficiency was increased when the flow rate was increased. From the interaction between the operations variables, they conclude that a maximum removal percentage of 68.63% is obtained with a bed height of 15 cm, a flow rate of 0.45 L/h and an initial RBOR concentration of 0.25 mmol/L. Regarding mathematical models, the authors indicate that RSM and ANFIS models can successfully predict removal efficiency with correlation coefficients of 0.9999 for the ANFIS model and 0.9981 for the RSM model.
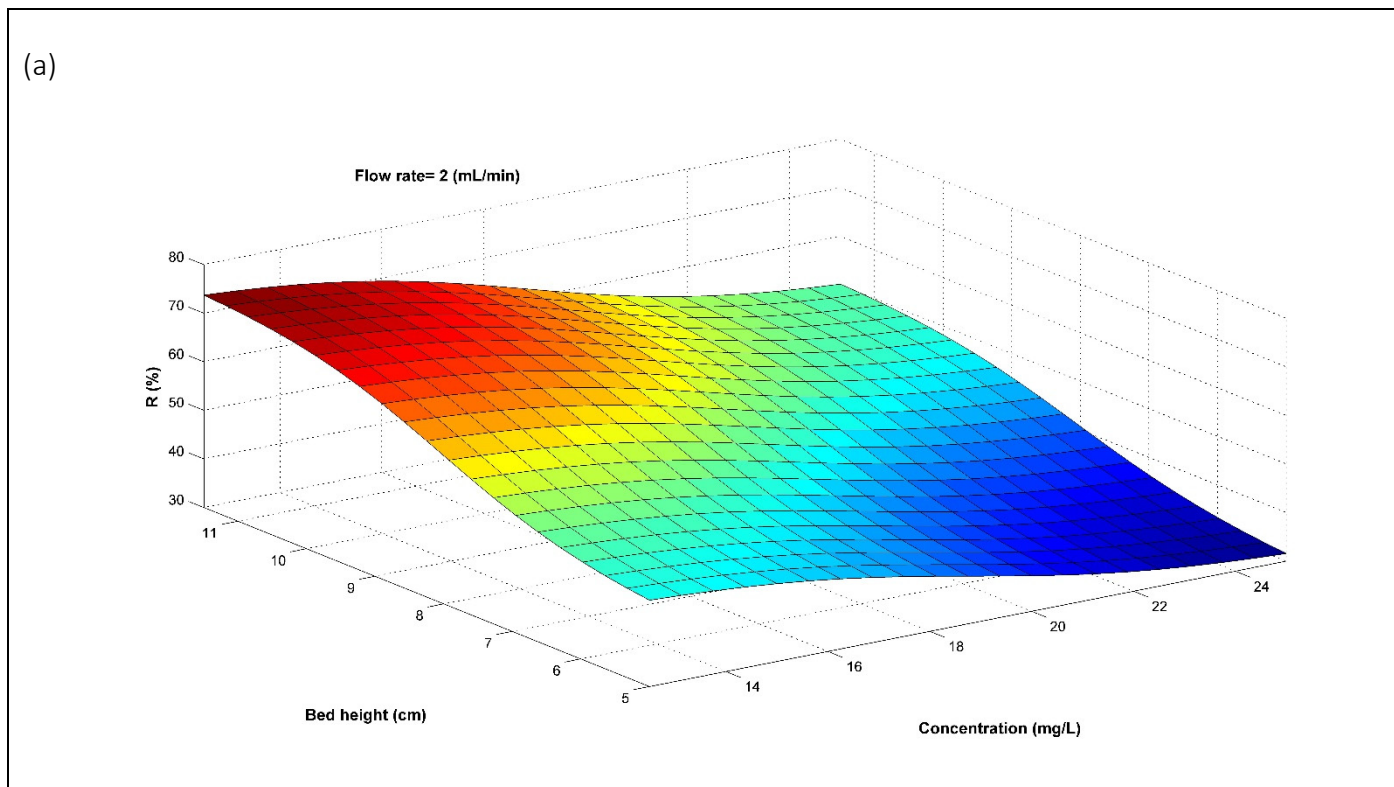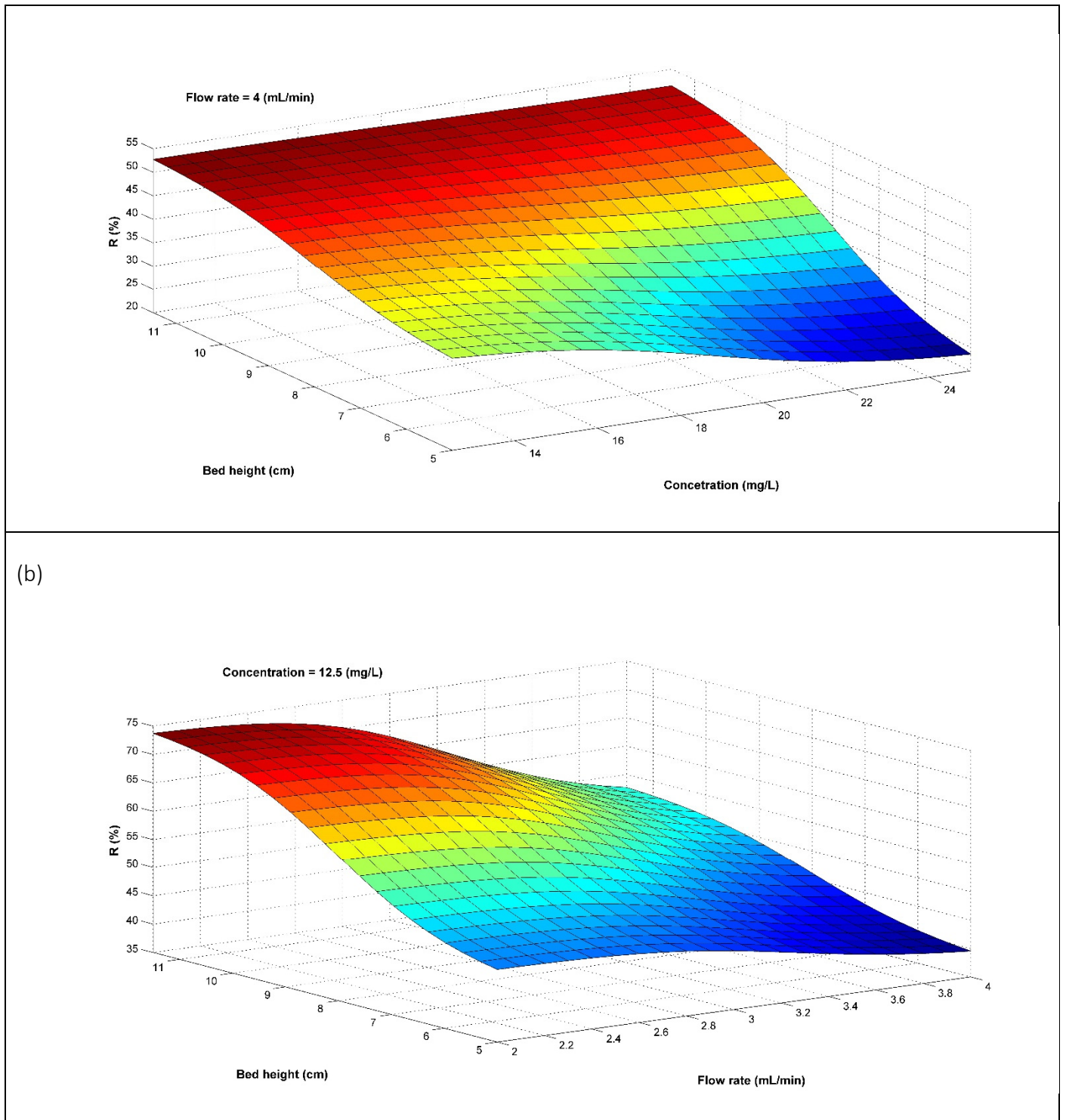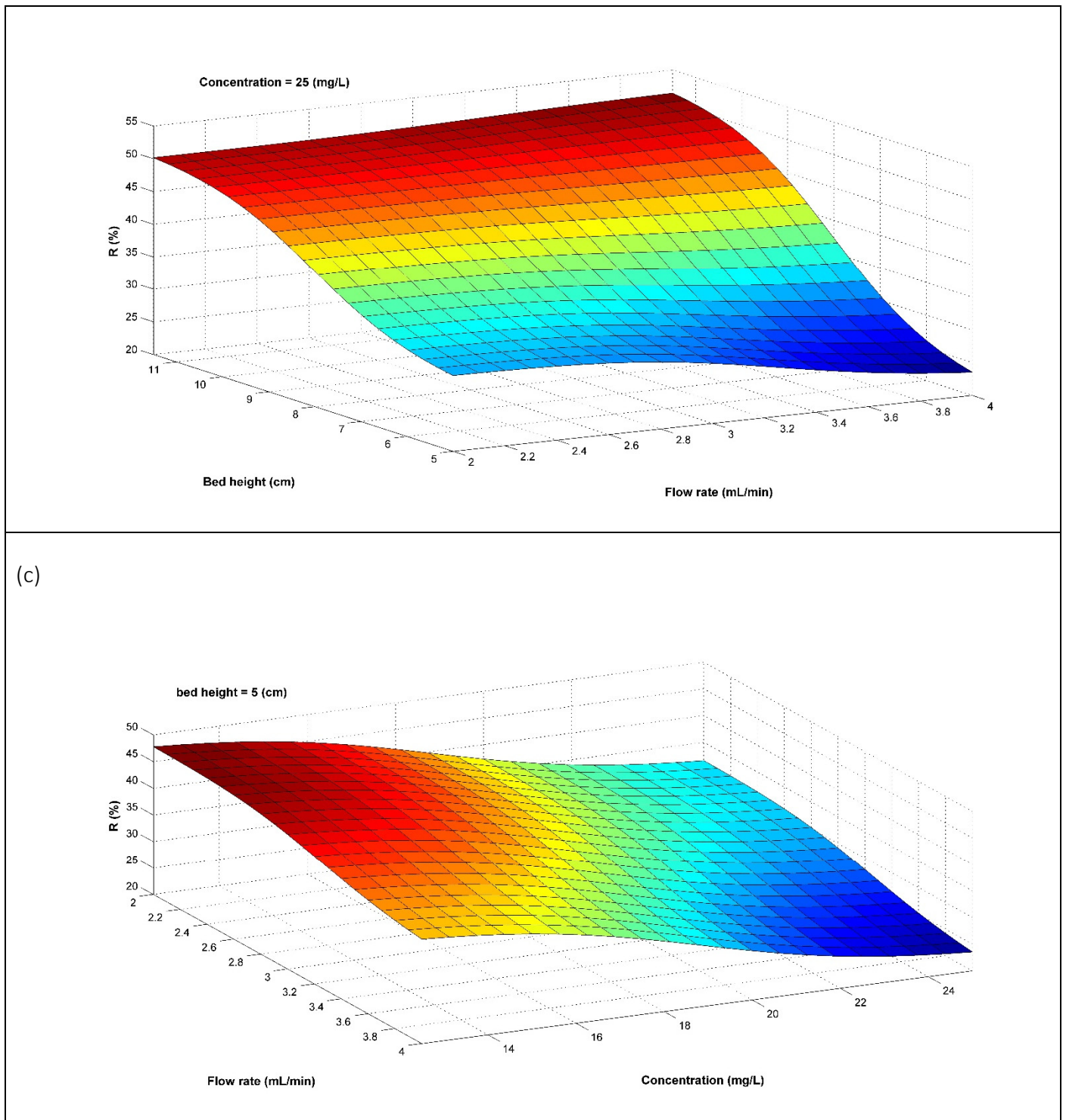

Figure 2. *Cont.*

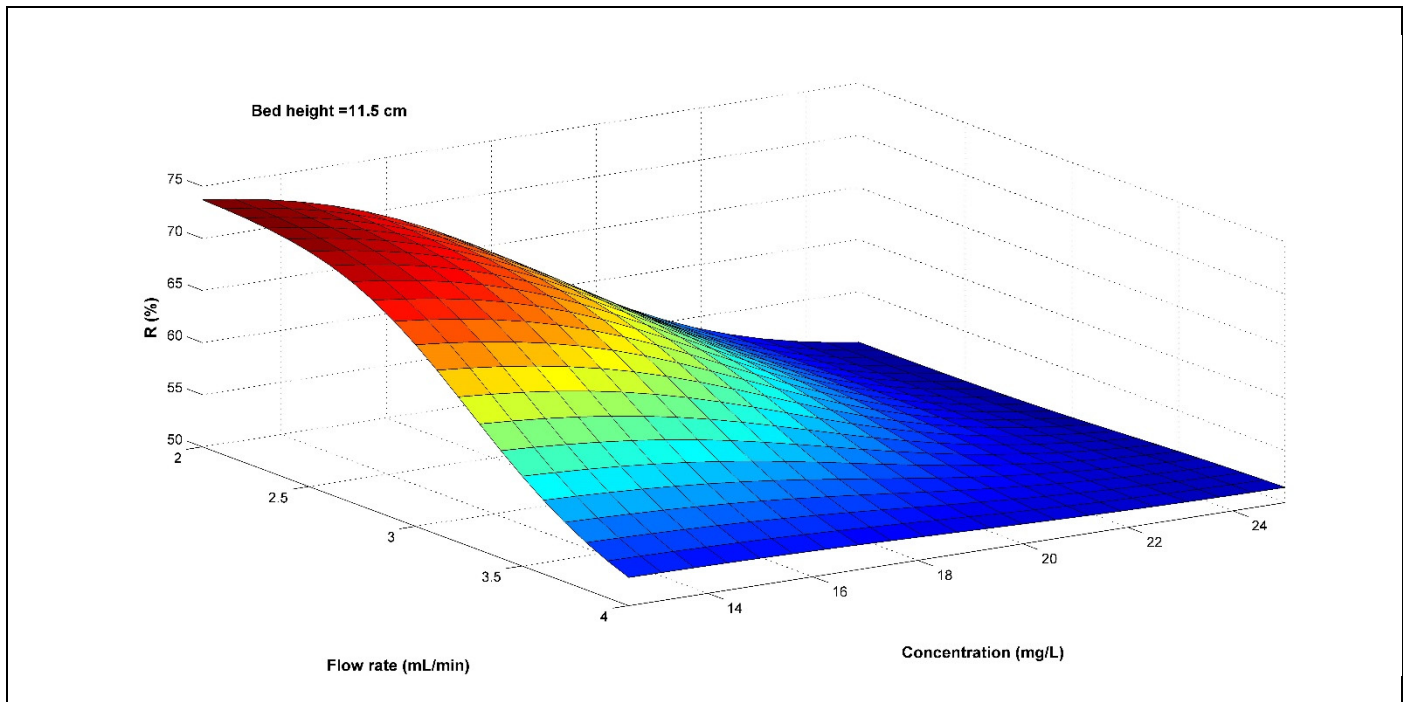**Figure 2.** *Cont*.

(c)

Figure 2. *Cont.*

Figure 2. Surface graphs for cobalt removal (%): (**a**) inlet concentration vs. bed height at constant feed-flow rate, (**b**) feed-flow rate vs. bed height at constant inlet concentration, (**c**) inlet concentration vs. feed-flow rate at constant bed height.
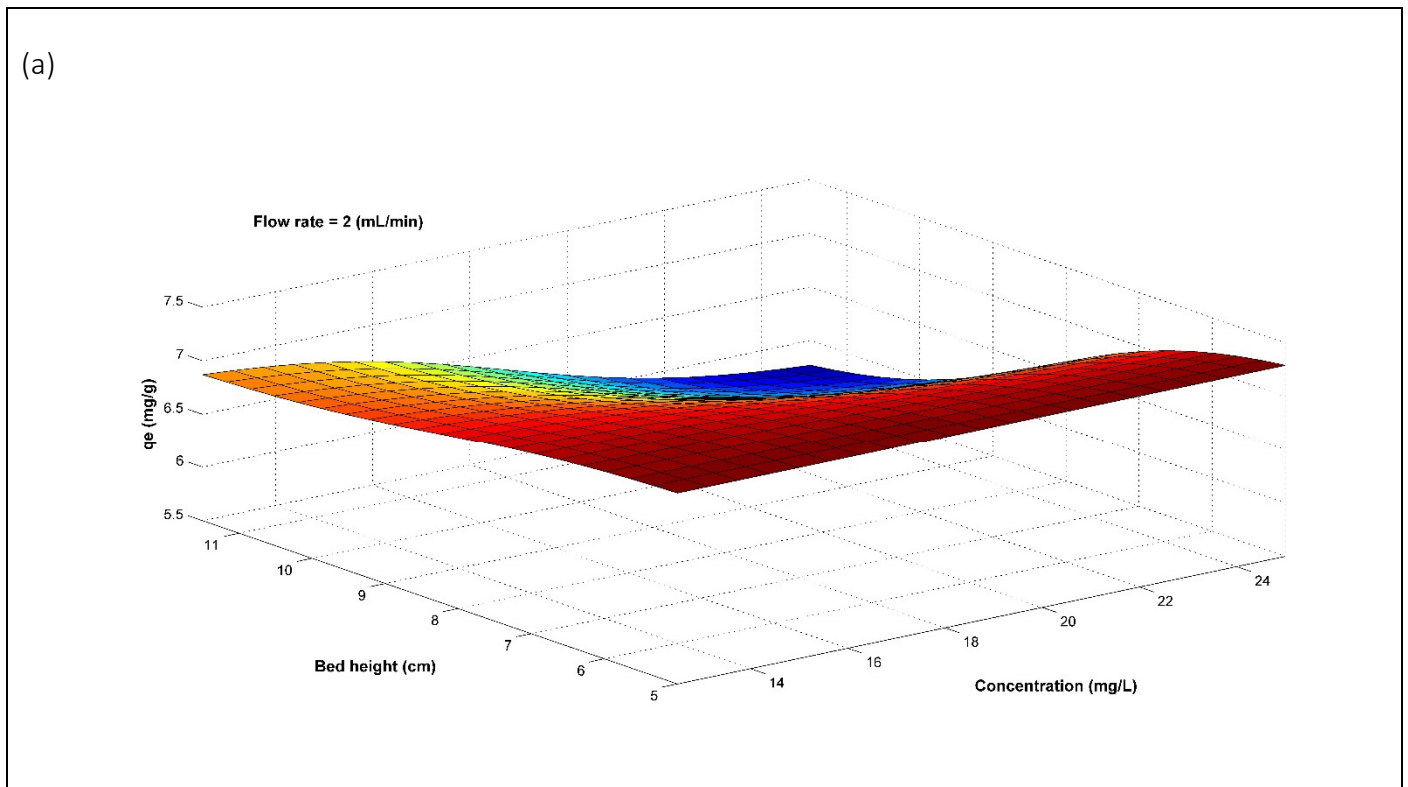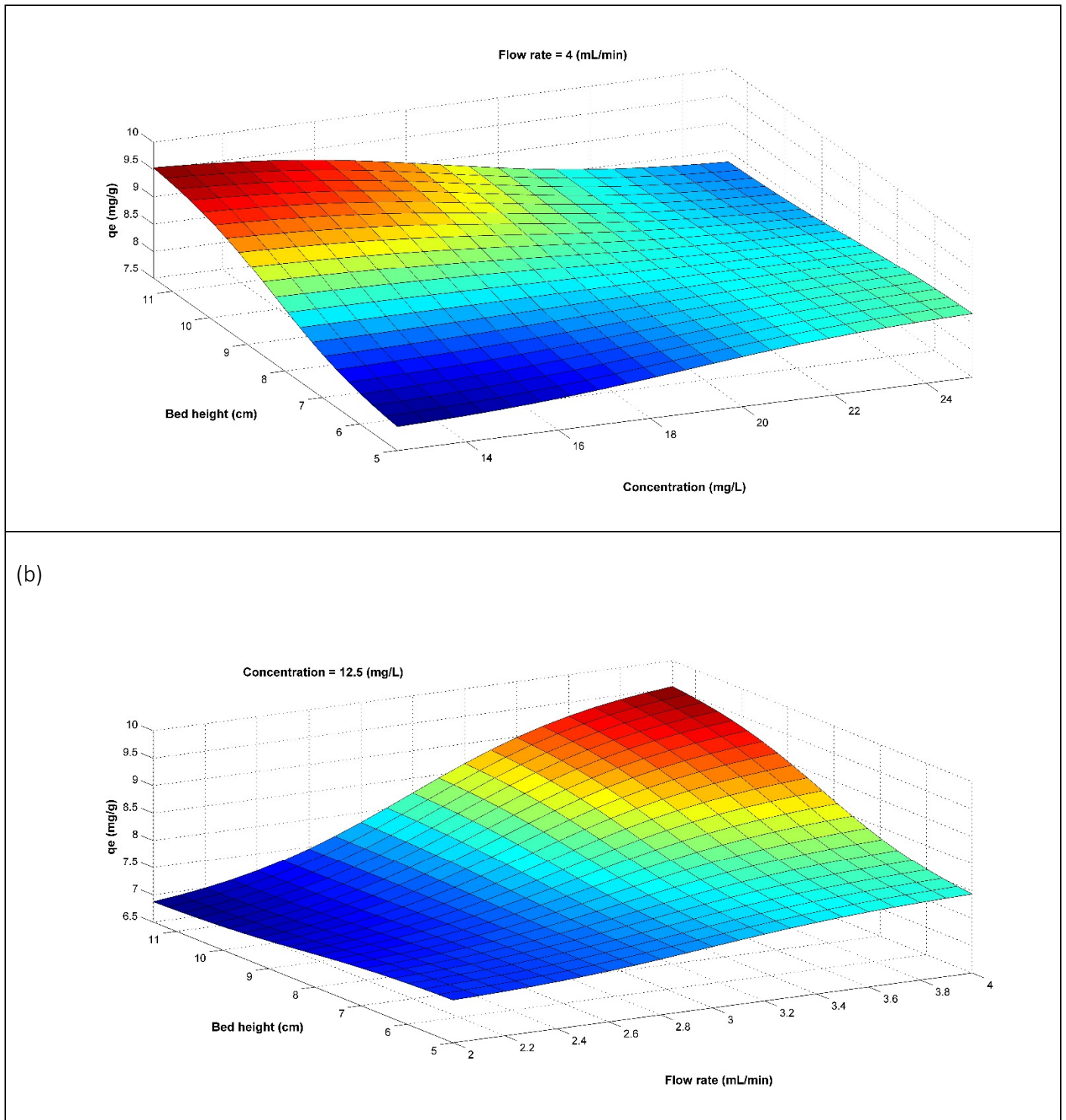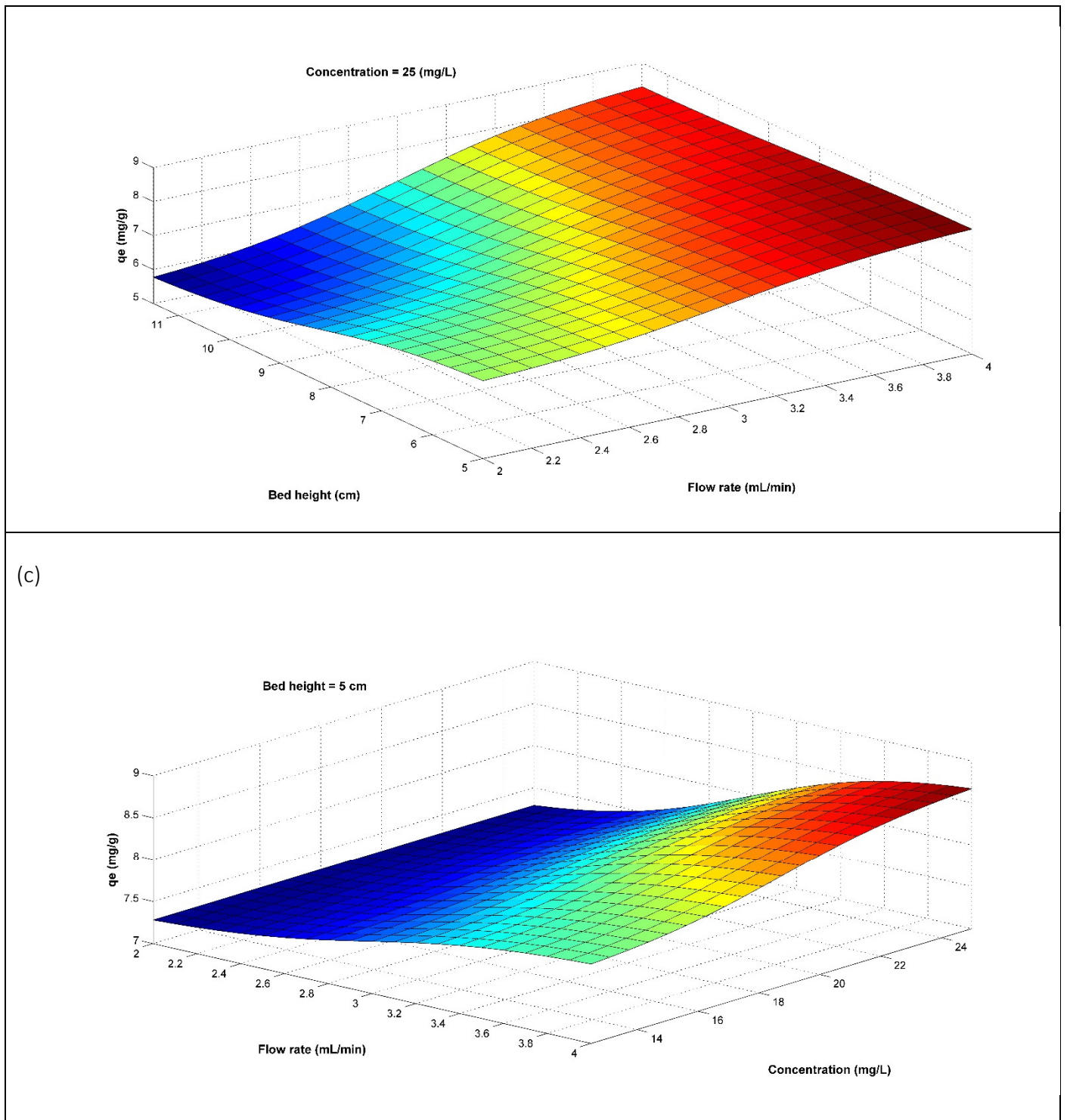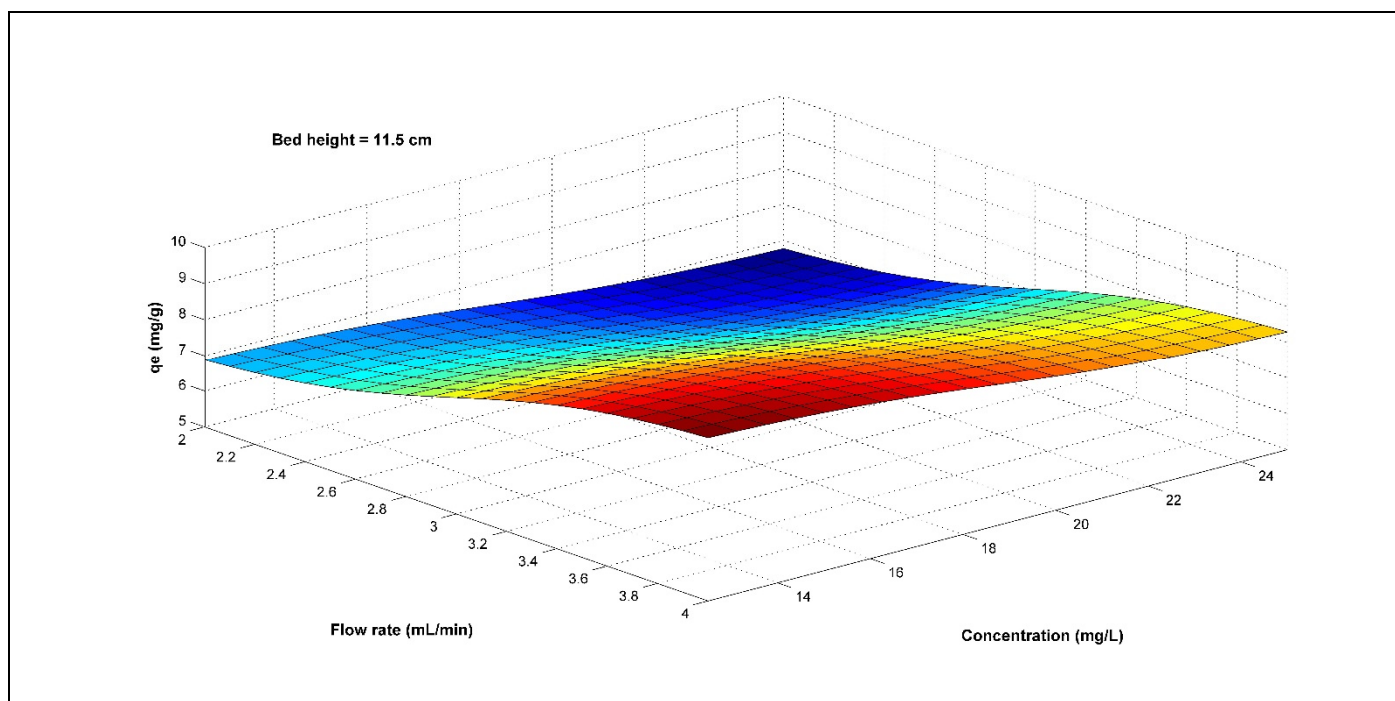

Figure 3. *Cont.*

Figure 3. *Cont.*

(c)

Figure 3. *Cont.*

Figure 3. Surface graphs for cobalt biosorption capacity (q_e): (**a**) inlet concentration vs. bed height at constant feed-flow rate, (**b**) feed-flow rate vs. bed height at constant inlet concentration, (**c**) inlet concentration vs. feed-flow rate at constant bed height.

Parsaei et al. [31] developed a model based on neural networks for the simulation of the Pb (II) and Cd (II) removal process using a new nanocomposite as adsorbent in a batch system. The authors indicate that the model fits the experimental data very well with R^2 values greater than 0.99. In addition, the authors indicate that the model showed that the initial solute concentration has a great influence on the percentage of adsorption, due to the change in the mass transfer rate and the driving force of the process. Similarly, Solanki et al., [32] applied ANFIS models to estimate the adsorption of hazardous azo dyes by a novel bionanocomposite with good statistical findings (R^2 values > 0.94; SSE < 0.4; MSE < 0.002; RMSE < 0.05). In addition, the application of ANFIS models were employed by Dolatabadi et al. [33] to optimize, create and develop prediction models for dye and Cu (II) adsorption by using sawdust from Melia Azedarach wood. These authors calculated an R^2 of 0.99 for both pollutants.

4. Conclusions

In this work, cobalt adsorption was studied using a novel biosorbent obtained from vegetal residues from intensive greenhouse crops. The results show that the variable that most affects the process is the feed flow. In general, an increase in the feed-flow rate caused an increase in the feed amount of cobalt and a decrease in the cobalt removal percentage. For example, for a concentration of 25 mg/L and a biosorbent mass of 1 g, the removal percentage decreased from 31.56% to 23.53% when the feed-flow rate increased from 2 to 4 mL/min. In addition, an increase in inlet cobalt concentration produced a reduction in the saturation time and increasing bed height produced an increase in saturation time, total amount of cobalt retained, and removal percentage of cobalt. The experimental and model outputs displayed acceptable results for ANFIS, providing R^2 values higher than 0.999 for both cobalt removal percentage and biosorption capacity. The most favorable operating conditions to maximize the removal percentage were 2 mL/min of feed-flow rate, 12.5 mg/L of inlet concentration and 11.5 cm of bed height and to maximize the biosoption

capacity were 4 mL/min feed-flow rate, 12.5 mg/L of inlet concentration and 11.5 cm of bed height.

References

1. Hossain, M.A.; Ngo, N.N.; Guo, W.S.; Nguyen, T.V.; Vigneswaran, S. Performance of cabbage and cauliflower wastes for heavy metals removal. *Desalin. Water Treat.* **2014**, *52*, 844–860. [CrossRef]

2. Abdolali, A.; Ngo, H.H.; Guo, W.; Zhou, J.L.; Zhang, J.; Liang, S.; Chang, S.W.; Nguyen, D.D.; Liu, Y. Application of a breakthrough biosorbent for removing heavy metals from synthetic and real wastewaters in a lab-scale continuous fixed-bed column. *Bioresour. Technol.* **2017**, *229*, 78–87. [CrossRef] [PubMed]

3. Cárdenas, J.F.; Rodríguez, A.S.; Vargas, J.M.; Martínez, V.M.; Acosta, I.; Michel, C.; Gallegos, F.; Escalera, M.E.; Muñoz, A. Bioremoval of Cobalt(II) from Aqueous Solution by Three Different and Resistant Fungal Biomasses. *Bioinorg. Chem. Appl.* **2019**, *2019*, 8757149. [CrossRef] [PubMed]

4. Lauwerys, R.; Lison, D. Health risks associated with cobalt exposure-an overview. *Sci. Total Environ.* **1994**, *150*, 1–6. [CrossRef]

5. Khan Rao, R.A.; Khatoon, A. Aluminate treated Casuarina equisetifolia leaves as potential adsorbent for sequestering Cu(II), Pb(II) and Ni(II) from aqueous solution. *J. Clean. Prod.* **2017**, *165*, 1280–1295. [CrossRef]

6. Chai, W.S.; Cheun, J.Y.; Jumar, P.S.; Mubashir, M.; Majeed, Z.; Banar, F.; Ho, S.-H.; Show, P.L. A review on conventional and novel materials towards heavy metal adsorption in wastewater treatment application. *J. Clean. Prod.* **2021**, *296*, 126589. [CrossRef]

7. Yelatontsev, D. Production of versatile biosorbent via eco-friendly utilization of non-wood biomass. *Chem. Eng. J.* **2023**, *451*, 13881. [CrossRef]

8. Quyen, V.T.; Pham, T.-H.; Kim, J.; Thanh, D.M.; Thang, P.Q.; Le, Q.V.; Jung, S.H.; Kim, T. Biosorbent derived from coffee husk for efficient removal of toxic heavy metals from wastewater. *Chemosphere* **2021**, *284*, 131312. [CrossRef]

9. Martín-Lara, M.A.; Blázquez, G.; Calero, M.; Almendros, A.I.; Ronda, A. Binary biosorption of copper and lead onto pine cone shell in batch reactors and in fixed bed columns. *Int. J. Miner. Process.* **2016**, *148*, 72–82. [CrossRef]

10. Calero, M.; Iáñez-Rodríguez, I.; Pérez, A.; Martín-Lara, M.A.; Blázquez, G. Neural fuzzy modelization of copper removal from wáter by biosorption in fixed-bed columns using olive stone a pinion shell. *Bioresour. Technol.* **2018**, *252*, 100–109. [CrossRef]

11. Ahmadi, H.; Hafiz, S.S.; Sharifi, H.; Rene, N.N.; Habibi, S.S.; Hussain, S. Low cost biosorbent (Melon Peel) for effective removal of Cu (II), Cd (II), and Pb (II) ions from aqueous solution. *Engineering* **2022**, *6*, 100242. [CrossRef]

12. Sankaran, R.; Show, P.L.; Ooi, C.-W.; Ling, T.C.; Shu-Jen, C.; Chen, S.-Y.; Chang, Y.-K. Feasibility assessment of removal of heavy metals and soluble microbial products from aqueous solutions using eggshell wastes. *Clean Technol. Environ. Policy* **2020**, *22*, 773–786. [CrossRef]

13. Kamarudzaman, A.I.; Adan, S.N.A.C.; Hassan, Z.; Wahab, M.A.; Makhtar, S.M.Z.; Seman, N.A.A.; Jalil, M.F.A.; Handayani, D.; Syafiuddin, A. Biosorption of Copper(II) and Iron(II) using Spent Mushroom Compost as Biosorbent. *Biointerface Res. Appl. Chem.* **2022**, *12*, 7775–7786.

14. Abdi, O.; Kazemi, M. A review study of biosorption of heavy metals and comparison between different biosorbents. *J. Mater. Environ. Sci.* **2015**, *6*, 1386–1399.

15. Morosanu, I.; Teodosiu, C.; Paduraru, C.; Ibanescu, D.; Tofan, L. Biosorption of lead ions from aqueous effluents by rapeseed biomass. *New Biotechnol.* **2017**, *39*, 110–124. [CrossRef] [PubMed]

16. Ronda, A.; Martín-Lara, M.A.; Almendros, A.I.; Pérez, A.; Blázquez, G. Comparison of two models for the biosorption of Pb (II) using untreated and chemically treated olive stone: Experimental design methodology and adaptive neural fuzzy inference system (ANFIS). *J. Taiwan Inst. Chem. Eng.* **2015**, *54*, 45–56. [CrossRef]

17. Fawzy, M.; Nasr, M.; Adel, S.; Nagy, H.; Helmi, S. Environmental approach and artificial intelligence for Ni (II) and Cd (II) biosorption form aqueous solution using Typha domingensis biomass. *Ecol. Eng.* **2016**, *95*, 743–752. [CrossRef]

18. Fawzy, M.; Nasr, M.; Helmi, S.; Nagy, H. Experimental and theoretical approaches for Cd (II) biosorption from aqueous solution using Oryza sativa biomass. *Int. J. Phytoremediat.* **2016**, *18*, 1096–1103. [CrossRef]

19. Bingöl, D.; Inal, M.; Çetintaş, S. Evaluation of copper biosorption onto date palm (Phoenix dactylifera L.) seeds with MLR and ANFIS models. *Ind. Eng. Chem. Res.* **2013**, *52*, 4429–4435. [CrossRef]

20. Jiménez, L.; Pérez, A.; de la Torre, M.J.; Rodríguez, A.; Angulo, V. Ethyleneglycol pulp from tagasaste. *Bioresour. Technol.* **2008**, *99*, 2170–2176. [CrossRef]

21. Iáñez-Rodríguez, I.; Martín-Lara, M.A.; Blázquez, G.; Pérez, A.; Calero, M. Effect of torrefaction conditions on greenhouse crop residue: Optimization of conditions to upgrade solid characteristics. *Bioresour. Tecnol.* **2017**, *244*, 741–749. [CrossRef] [PubMed]

22. Basu, A.; Ali, S.S.; Hossain, S.S.; Asif, M. A review of the dynamic mathematical modeling of heavy metal removal with the biosorption process. *Processes* **2022**, *10*, 1154. [CrossRef]

23. Chen, S.; Yue, Q.; Gao, B.; Li, Q.; Xu, X.; Fu, K. Adsorption of hexavalent chromium from aqueous solution by modified corn stalk: A fixed-bed column study. *Bioresour. Technol.* **2012**, *113*, 114–120. [CrossRef] [PubMed]

24. Sheng, L.; Zhang, Y.; Tang, F.; Liu, S. Mesoporous/microporous silica materials: Preparation from natural sands and highly efficient fixed-bed adsorption of methylene blue in wastewater. *Microporous Mesoporous Mater.* **2018**, *257*, 9–18. [CrossRef]

25. Amin, M.T.; Alazba, A.A.; Shafiq, M. Batch and fixed-bed column studies for the biosorption of Cu(II) and Pb(II) by raw and treated date palm leaves and orange peel. *Glob. NEST J.* **2017**, *19*, 464–478.

26. Hymavathi, D.; Prabhakar, G. Modeling of cobalt and lead adsorption by Ficusbenghalenesis L in a fixed bed column. *Chem. Eng. Commun.* **2019**, *206*, 1264–1272. [CrossRef]

27. Rusu, L.; Grigoras, C.-G.; Simion, A.-I.; Suceveanu, E.-M.; Botezatu, A.V.D.; Harja, M. Biosorptive Removal of Ethacridine Lactate from Aqueous Solutions by Saccharomyces pastorianus Residual Biomass/Calcium Alginate Composite Beads: Fixed-Bed Column Study. *Materials* **2022**, *15*, 4657. [CrossRef]

28. Yahya, M.D.; Abubakar, H.; Obayomi, K.S.; Iyaka, Y.A.; Suleiman, B. Simultaneous and continuous biosorption of Cr and Cu (II) ions from industrial tannery effluent using almond shell in a fixed bed column. *Results Eng.* **2020**, *6*, 100113. [CrossRef]

29. Homem, N.C.; Vieira, A.M.S.; Bergamasco, R.; Vieira, M.F. Low-cost biosorbent based on Moringa oleifera residues for herbicide atrazine removal in a fixed-bed column. *Can. J. Chem. Eng.* **2018**, *96*, 1468–1478. [CrossRef]

30. Hanumanthu, J.R.; Ravindiran, G.; Subramanian, R.; Saravanan, P. Optimization of process conditions using RSM and ANFIS for the removal of Remazol Brilliant Orange 3R in a packed bed column. *J. Indian Chem. Soc.* **2021**, *98*, 100086. [CrossRef]

31. Parsaei, M.; Roudbari, E.; Piri, F.; El-Shafay, A.S.; Su, C.-H.; Nguyen, H.C.; Alashwa, M.; Ghazali, S.; Algarni, M. Neural-based modeling adsorption capacity of metal organic framework materials with application in wastewater treatment. *Sci. Rep.* **2022**, *12*, 4125. [CrossRef] [PubMed]

32. Solanki, S.; Sinha, S.; Bisaria, K.; Singh, R.; Saxena, R. Accurate data prediction by fuzzy inference model for adsorption of hazardous azo dyes by novel algal doped magnetic chitosan bionanocomposite. *Environ. Res.* **2022**, *214*, 113844. [CrossRef] [PubMed]

33. Dolatabadi, M.; Mehrabpour, M.; Esfandayari, M.; Alidadi, H.; Davoudi, M. Modeling of simultaneous adsorption of dye and metal ion by sawdust from aqueous solution using of ANN and ANFIS. *Chemom. Intell. Lab. Syst.* **2018**, *181*, 72–78. [CrossRef]